



LUND UNIVERSITY

New spectroscopic information on $^{211,213}\text{Tl}$

A changing structure beyond the $N=126$ shell closure

Gottardo, A.; Valiente-Dobón, J. J.; Benzoni, G.; Morales, A. I.; Gadea, A.; Lunardi, S.; Boutachkov, P.; Bruce, A. M.; Górska, M.; Grebosz, J.; Pietri, S.; Podolyák, Zs; Pfützner, M.; Regan, P. H.; Rudolph, D.; Weick, H.; Alcántara Núñez, J.; Algora, A.; Al-Dahan, N.; De Angelis, G.; Ayyad, Y.; Alkhomashi, N.; Allegro, P. R.P.; Bazzacco, D.; Benlliure, J.; Bowry, M.; Bracco, A.; Bunce, M.; Camera, F.; Casarejos, E.; Cortes, M. L.; Crespi, F. C.L.; Corsi, A.; Denis Bacelar, A. M.; Deo, A. Y.; Domingo-Pardo, C.; Doncel, M.; Dombradi, Zs; Engert, T.; Eppinger, K.; Farrelly, G. F.; Farinon, F.; Geissel, H.; Gerl, J.; Goel, N.; Gregor, E.; Habermann, T.; Hoischen, R.; Janik, R.; Klupp, S.

Published in:
Physical Review C

DOI:
[10.1103/PhysRevC.99.054326](https://doi.org/10.1103/PhysRevC.99.054326)

2019

Document Version:
Publisher's PDF, also known as Version of record

[Link to publication](#)

Citation for published version (APA):

Gottardo, A., Valiente-Dobón, J. J., Benzoni, G., Morales, A. I., Gadea, A., Lunardi, S., Boutachkov, P., Bruce, A. M., Górska, M., Grebosz, J., Pietri, S., Podolyák, Z., Pfützner, M., Regan, P. H., Rudolph, D., Weick, H., Alcántara Núñez, J., Algora, A., Al-Dahan, N., ... Maglione, E. (2019). New spectroscopic information on $^{211,213}\text{Tl}$: A changing structure beyond the $N=126$ shell closure. *Physical Review C*, 99(5), Article 054326. <https://doi.org/10.1103/PhysRevC.99.054326>

Total number of authors:
81

General rights

Unless other specific re-use rights are stated the following general rights apply:
Copyright and moral rights for the publications made accessible in the public portal are retained by the authors and/or other copyright owners and it is a condition of accessing publications that users recognise and abide by the legal requirements associated with these rights.

- Users may download and print one copy of any publication from the public portal for the purpose of private study or research.
- You may not further distribute the material or use it for any profit-making activity or commercial gain
- You may freely distribute the URL identifying the publication in the public portal

Read more about Creative commons licenses: <https://creativecommons.org/licenses/>

Take down policy

If you believe that this document breaches copyright please contact us providing details, and we will remove access to the work immediately and investigate your claim.

Download date: 18. May. 2025

LUND UNIVERSITY

PO Box 117
221 00 Lund
+46 46-222 00 00

New spectroscopic information on $^{211,213}\text{Tl}$: A changing structure beyond the $N = 126$ shell closure

A. Gottardo,^{1,2,*} J. J. Valiente-Dobón,¹ G. Benzoni,³ A. I. Morales,³ A. Gadea,⁴ S. Lunardi,^{2,5} P. Boutachkov,⁶ A. M. Bruce,⁷ M. Górska,⁶ J. Grebosz,⁸ S. Pietri,⁶ Zs. Podolyák,⁹ M. Pfützner,¹⁰ P. H. Regan,⁹ D. Rudolph,¹¹ H. Weick,⁶ J. Alcántara Núñez,¹² A. Algora,⁴ N. Al-Dahan,⁹ G. de Angelis,¹ Y. Ayyad,¹² N. Alkhomashi,¹³ P. R. P. Allegro,¹⁴ D. Bazzacco,⁵ J. Benlliure,¹⁵ M. Bowry,⁹ A. Bracco,^{3,16} M. Bunce,⁷ F. Camera,^{3,16} E. Casarejos,¹⁷ M. L. Cortes,⁶ F. C. L. Crespi,³ A. Corsi,^{3,16} A. M. Denis Bacelar,⁷ A. Y. Deo,⁹ C. Domingo-Pardo,⁶ M. Doncel,¹⁸ Zs. Dombradi,¹⁹ T. Engert,⁶ K. Eppinger,²⁰ G. F. Farrelly,⁹ F. Farinon,⁶ H. Geissel,⁶ J. Gerl,⁶ N. Goel,⁶ E. Gregor,⁶ T. Habermann,⁶ R. Hoischen,^{6,11} R. Janik,²¹ S. Klupp,²⁰ I. Kojouharov,⁶ N. Kurz,⁶ S. M. Lenzi,^{2,5} S. Leoni,^{3,16} S. Mandal,²² R. Menegazzo,⁵ D. Mengoni,⁵ B. Million,³ D. R. Napoli,¹ F. Naqvi,^{6,23} C. Nociforo,⁶ A. Prochazka,⁶ W. Prokopowicz,⁶ F. Recchia,⁵ R. V. Ribas,¹⁴ M. W. Reed,⁹ E. Sahin,¹ H. Schaffner,⁶ A. Sharma,⁶ B. Sitar,²¹ D. Siwal,²² K. Steiger,²⁰ P. Strmen,²¹ T. P. D. Swan,⁹ I. Szarka,²¹ C. A. Ur,⁵ P. M. Walker,^{9,24} O. Wieland,³ H.-J. Wollersheim,⁶ F. Nowacki,²⁵ and E. Maglione²⁶

¹Istituto Nazionale di Fisica Nucleare, Laboratori Nazionali di Legnaro, Legnaro 35020, Italy

²Dipartimento di Fisica dell'Università degli Studi di Padova, Padova 35131, Italy

³Istituto Nazionale di Fisica Nucleare, Sezione di Milano, Milano 20133, Italy

⁴Instituto de Física Corpuscular, CSIC-Universitat de València, València E-46980, Spain

⁵Istituto Nazionale di Fisica Nucleare, Sezione di Padova, Padova 35131, Italy

⁶GSI Helmholtzzentrum für Schwerionenforschung, Darmstadt D-64291, Germany

⁷School of Computing, Engineering and Mathematics, University of Brighton, Brighton BN2 4GJ, United Kingdom

⁸Niewodniczanski Institute of Nuclear Physics, Polish Academy of Science, Krakow PL-31-342, Poland

⁹Department of Physics, University of Surrey, Guildford GU2 7XH, United Kingdom

¹⁰Faculty of Physics, University of Warsaw, Warsaw PL-00681, Poland

¹¹Department of Physics, Lund University, Lund S-22100, Sweden

¹²Universidade de Santiago de Compostela, Santiago de Compostela E-175706, Spain

¹³KACST, Riyadh 11442, Saudi Arabia

¹⁴Instituto de Física, Universidade de São Paulo, São Paulo 05315-970, Brazil

¹⁵IGFAE, Universidade de Santiago de Compostela, Santiago de Compostela E-15782, Spain

¹⁶Dipartimento di Fisica dell'Università degli Studi di Milano, Milano 20133, Italy

¹⁷EEL, Universidade de Vigo, Vigo E-36310, Spain

¹⁸Grupo de Física Nuclear, Universidad de Salamanca, Salamanca E-37008, Spain

¹⁹Institute of Nuclear Research of the Hungarian Academy of Sciences, Debrecen H-4001, Hungary

²⁰Physik Department, Technische Universität München, Garching D-85748, Germany

²¹Faculty of Mathematics and Physics, Comenius University, Bratislava 84215, Slovakia

²²Department of Physics and Astrophysics, University of Delhi, Delhi 110007, India

²³Institut für Kernphysik, Universität zu Köln, Köln D-50937, Germany

²⁴CERN, Geneva CH-1211, Switzerland

²⁵Université de Strasbourg, IPHC, 23 rue du Loess and CNRS, UMR7178, Strasbourg 67037, France

²⁶Departamento de Física, Instituto Superior Técnico, Universidade de Lisboa, Lisbon, Portugal



(Received 14 February 2019; published 23 May 2019)

The neutron-rich isotopes $^{211,213}\text{Tl}$, beyond the $N = 126$ shell closure, have been studied for the first time in isomer γ -ray decay, exploiting the fragmentation of a primary uranium beam at the Fragment Separator-Rare Isotopes Investigation at GSI setup. The observed isomeric states in $^{211,213}\text{Tl}$ show a deviation from the seniority-like scheme of ^{209}Tl . The possible interpretation of the data is discussed on the basis of energy-level systematics and shell-model calculations.

DOI: [10.1103/PhysRevC.99.054326](https://doi.org/10.1103/PhysRevC.99.054326)

* andrea.gottardo@lnl.infn.it

I. INTRODUCTION

Published by the American Physical Society under the terms of the [Creative Commons Attribution 4.0 International](https://creativecommons.org/licenses/by/4.0/) license. Further distribution of this work must maintain attribution to the author(s) and the published article's title, journal citation, and DOI.

Doubly-magic nuclei constitute the cornerstones of our knowledge of nuclear structure. Indeed, isotopes around shell closures exhibit excitations which have a single-particle nature sufficiently strong to be indicative of the shell-gap size and of the energies of shells above or below the doubly-magic core. Given the limited number of nucleons outside an

a priori inert core, regions around doubly-magic nuclei are also readily accessible to shell-model calculations, including the possibility of considering particle-hole excitations across the core. As a consequence, a great number of studies have concentrated on regions around doubly-magic nuclei. For the neutron-rich heavy nuclei ^{132}Sn and ^{208}Pb , the investigation of the isotopes beyond $N = 82$ and below $Z = 50$ and beyond $N = 126$ and below $Z = 82$, respectively, has been hampered by their exotocity. In particular, in the case of ^{208}Pb , these neutron-rich isotopes can be reached only by cold fragmentation from ^{238}U at the present facilities, while the future availability of reaccelerated radioactive ion beams may make them reachable also by multinucleon transfer reactions. The region beyond $N = 126$ and below $Z = 82$ is possibly one of the least explored quadrants of the Segré chart. Preliminary studies have concerned mainly mercury isotopes, with spectroscopic studies on ^{208}Hg and ^{210}Hg conducted by means of isomer decay. While in the $N = 128$ ^{208}Hg isotope a seniority-scheme-like structure is observed [1], similarly to lead isotopes [2], in ^{210}Hg the spectrum exhibits some differences [3]. Besides the expected $I^\pi = 8^+$ seniority isomer, another low-lying isomeric state appears. Although its spin and parity could not be firmly assigned, a low-lying collective 3^- state was proposed. However, theoretical models do not predict such a low energy for a 3^- state in ^{210}Hg , leaving the issue of the nature of this second isomeric state open until now. In this regard, a spectroscopic study of thallium isotopes beyond $N = 126$ could shed some light and show whether a structure other than the seniority schemes of $^{210-216}\text{Pb}$ is developing or not.

Due to the low production cross sections of these heavy exotic nuclei, only the $N = 128$ ^{209}Tl nucleus was studied beyond the $N = 126$ shell closure. It was first observed in a (t, α) reaction on a radioactive ^{210}Pb target [4]. A more complete spectroscopic information was obtained in the aforementioned isomer-decay ^{208}Hg experiment [1]. More recently, a multinucleon transfer reaction with a ^{208}Pb target managed to collect prompt and delayed γ -spectroscopy data on ^{209}Tl [5]. Other β -decay studies were also performed in the past [6–9]. The experiment object of this paper also conveyed useful new information on the β decay in this region probing the role of first-forbidden decays across $N = 126$ [10,11]. Attempts to populate heavy nuclei around ^{208}Pb nuclei have also been made using spallation reactions of 1.4-GeV protons on a UCx target at ISOLDE [12].

The present paper reports on a γ -ray isomer decay study of $N = 130, 132, ^{211,213}\text{Tl}$ isotopes. The paper is organized as follows. The experimental set-up is described in the first section, while γ -ray spectroscopy results are shown in the second section. The third section will deal with the discussion of the results with the help of shell-model calculations.

II. EXPERIMENTAL SETUP

Neutron-rich nuclei in the lead region are primarily accessible via cold fragmentation of a ^{238}U beam. The heavy mass (>200) of the isotopes involved implies a number of technical difficulties concerning primarily Z identification of the reaction products as well as charge state transportation and separation in the mass spectrometer [13]. These difficulties can be, at

least partially, overcome with a high primary beam energy and a dedicated setup. The coupling of the UNILAC-SIS18 accelerator facilities at GSI with the FRagment Separator-Rare ISotopes INvestigation at GSI (FRS-RISING) experimental complex [14–17] constitutes a unique setup to study neutron-rich heavy nuclei beyond $N = 126$ around ^{208}Pb . The isotopes of interest were produced exploiting the fragmentation of a 1 GeV/nucleon ^{238}U beam, with an intensity of around 1.5×10^9 ions/spill. The ~ 1 s beam extraction spills were separated by a ~ 2 s period without beam. The uranium ions underwent fragmentation reactions on a 2.5 g/cm^2 Be target, which was followed by a 223-mg/cm^2 Nb stripper to improve the number of fully stripped ions. The resulting reaction fragments were separated according to their magnetic rigidity ($B\rho$) with the double-stage magnetic spectrometer FRS [14].

A significant challenge was the necessity to reject the primary beam charge states, which would otherwise induce a too high counting rate at the intermediate focal plane S2, where the first particle detectors along the FRS beam line are placed. A similar problem was presented by the strongly produced Rn and Ra isotopes, which would also generate an unsustainable counting rate of $\sim 10^8$ Hz on the available detectors. This problem was handled by implementing a preseparation of reaction products and primary beam in the first stage of the FRS. A homogeneous 2-g/cm^2 Al degrader was placed after the first dipole of the FRS in order to exclude heavy fragments above polonium ($Z > 84$) from its acceptance, thanks to the change of their magnetic rigidity.

The second stage of the FRS was used to perform a more refined separation in $B\rho$, using the $B\rho - \Delta E - B\rho$ method to further purify the radioactive cocktail beam [14–17]. This was achieved with help of a wedge-shaped 758-mg/cm^2 Al degrader placed at the S2 focal plane, with an angle set to produce a monochromatic beam at the end of the FRS. The $B\rho$ was determined by measuring focal-plane positions with Time-Projection Chamber detectors. The time-of-flight (TOF) was measured from plastic scintillators at the S2 and the final focal S4 planes. The mass-over-charge ratio A/Q (A/Z in the case of fully stripped ions) could then be determined from the $B\rho$ and TOF measurements on an event-by-event basis. The atomic number, Z , of the fragments was obtained from the energy loss in two ionization chambers placed at the S4 final focal plane.

This experimental technique allowed an unambiguous determination of the mass and atomic number of fully stripped ions. The possible change in the ion charge state when passing through the degrader and detector materials was dealt with by comparing the $B\rho$ before and after the Al wedge-shaped degrader. The events showing a change in the charge state were excluded from the subsequent analysis. Figure 1 shows the typical identification plot obtained from analysis. The separation in both Z and $A/(Q = Z)$ ratio is sufficient not to suffer from contamination from neighboring isotopes.

Since the aim was to perform decay spectroscopy of the exotic cocktail beam from FRS, at the S4 final focal plane the ions were slowed down in a thick Al degrader to obtain an energy suitable for implantation in the three layers of a double-sided silicon-strip (DSSSD) detector system placed

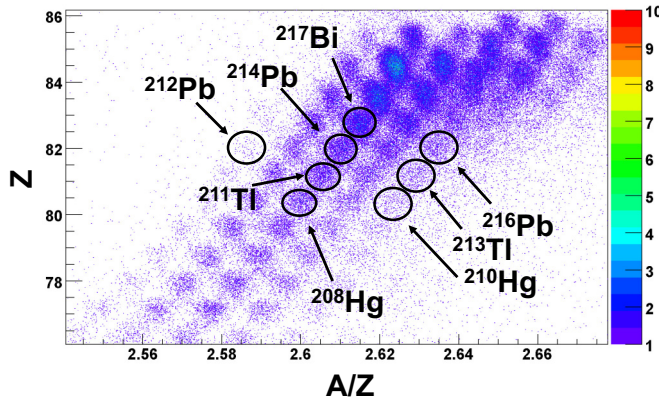


FIG. 1. Reaction fragment identification plot at the final focal plane of the FRS. The fragments of interest have been circled, as well as some neighboring nuclei to provide a reference.

after the degrader. Each layer was composed of three DSSSD pads [17,18]. The monochromatic energy structure of the beam ensured that the implantation depth in the active stopper was the same for all the fragments of a given A/Z and Z . The DSSSD detector system was placed at the center of the RISING γ spectrometer, consisting of 105 germanium crystals arranged in 15 clusters with 7 crystals each [15,16]. The full-energy γ -ray peak detection efficiency of the array was measured to be 15% at 662 keV [15]. The time correlation between the γ rays and the ions detected by the active stopper allowed one to perform at the same time isomer spectroscopy and β -delayed γ -ray spectroscopy [10,11]. The isomer spectroscopy studies are affected by the presence of a prompt flash of γ rays during the implantation of heavy ions. This prompt flash extends in time several tens of ns for low γ -ray energies around 100–200 keV, due to the RISING detectors time resolution and walk time. Therefore, it is necessary to search for possible isomer γ -ray decays in a time window starting several hundred ns after the implantation event, limiting the sensitivity for isomers with short lifetimes, below 100 ns.

III. EXPERIMENTAL RESULTS

A. ^{211}Tl

Figure 2 shows the γ -ray spectrum obtained for ^{211}Tl with a time period 0.12–3.00 μs between ion implantation and γ -ray detection. One transition at 144 keV dominates the spectrum, with no other γ lines visible. Longer (up to 400 μs) and shorter (down to 40 ns) time windows have been attempted, but no additional transitions were found.

A $\gamma\gamma$ coincidence spectrum was also built from data. The coincidences (within a 100 ns time window) with the 144-keV γ ray are illustrated in Fig. 3, which shows no peak. Table I reports the area of the 144-keV transition with the associated uncertainty. The time distribution of the γ ray was fitted with an exponential curve, as shown in Fig. 4 to derive a half-life of $t_{1/2} = 0.58 \pm 0.08 \mu\text{s}$. The error is the quadratical sum of the statistical uncertainty derived from the fit and of systematic errors linked to binning and interval of the fit.

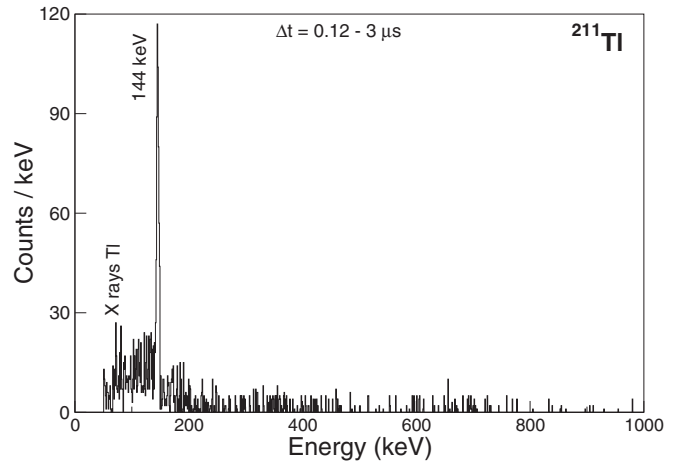


FIG. 2. Gamma-ray spectrum from the decay of the isomeric state in ^{211}Tl . The spectrum has been taken with a time window 0.12–3.00 μs after implantation.

B. ^{213}Tl

Figure 5 shows the γ -ray spectrum obtained for ^{213}Tl with a time window of 0.12–20.00 μs : Two γ -ray transitions appear at 380 and 698 keV. Figure 6 shows that these two γ rays appear not to be in prompt coincidence. Table II reports the areas of the two γ lines. The time distributions of the γ rays were least-squares fitted with an exponential curve, see Figs. 7 and 8, to derive a half-life of $t_{1/2} = (4.1 \pm 0.5) \mu\text{s}$ for the 380-keV line and of $t_{1/2} = (0.6 \pm 0.3) \mu\text{s}$ for the 698-keV γ ray. They are not compatible, possibly indicating the existence of two isomers. Uncertainty on lifetimes was estimated as for the ^{211}Tl case.

IV. DISCUSSION

We start by briefly recalling the interpretation of the observed ^{209}Tl level scheme [12]. The basic idea is that the proton hole in the $Z = 82$ shell closure (mainly in the $d_{3/2}$ and $s_{1/2}$ orbits) couples to the seniority-isomer structure observed in ^{210}Pb . Calculations were therefore performed in a model space constituted by the $g_{9/2}$, $i_{11/2}$, $j_{15/2}$ orbits for neutrons above $N = 126$, and the $d_{5/2}$, $d_{3/2}$, $h_{11/2}$, $s_{1/2}$ orbits for the proton space below $Z = 82$. No excitations across the $Z = 82$ and $N = 126$ cores are thus included. The neutron-neutron

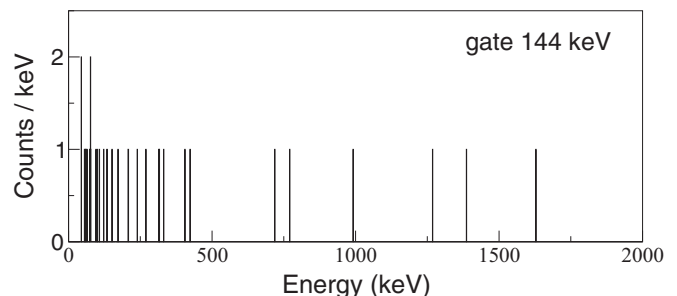


FIG. 3. Gamma-ray spectrum in prompt coincidence with the 144-keV transition from the decay from the isomeric state in ^{211}Tl .

TABLE I. Ratio between the ^{211}Tl 144(1) keV γ -ray intensity corrected for efficiency and electron conversion, in the hypothesis of an $E2$ transition, and the number of implanted ^{211}Tl ions. The errors on the corrected area are statistical ones quadratically summed to a relative 10% uncertainty in the efficiency calibration.

γ energy (keV)	Area	Area corrected/number of ions
144 (1)	474 (32)	0.21 (3)

and proton-proton matrix elements are from the Kuo-Herling interaction [19], while the proton-neutron matrix elements have been deduced from the bare H7B G matrix [20], without core polarization, as explained in Ref. [19]. The only change made to the Hamiltonian is to increase the matrix element $(\nu g_{9/2})_{8^+}^2$ by 40 keV to get the correct ordering of 6^+ and 8^+ states in ^{208}Hg , as suggested in Ref. [1]. Therefore, the wave functions of the holes in the proton core will mainly be constituted by the $s_{1/2}$ and $d_{3/2}$ orbits, while the particle wave function for neutrons will be dominantly $(g_{9/2})^n$, as in the case of the lead isotopes [2]. The effective charges used for neutrons and protons are $0.8e$ and $1.5e$, respectively. The effective charge for neutrons is increased from the usual $0.5e$ value for the ^{208}Pb region [2] to $0.8e$, because the neutron valence space has been truncated to only three shells for the thallium isotopes, which was necessary to keep the Hamiltonian matrix dimensions at a feasible level. Figure 9 reports the comparison between the experimental level scheme observed in Refs. [1] and our calculations performed with ANTOINE [21,22]. The $5/2^+$ state was observed in Ref. [5]. As claimed in Ref. [1], the agreement is quite good for energies for both ^{209}Tl and ^{208}Hg . At the time of that work, the $5/2^+$ state had not been observed yet. Concerning the $17/2^+$ seniority-isomer lifetime, the shell-model $B(E2 : 17/2^+ \rightarrow 13/2^+)$ value is $50 e^2 \text{ fm}^4$, smaller than the measured $129(20) e^2 \text{ fm}^4$ [1]. The aforementioned calculations predict that the $17/2^+$ isomer results, at a percentage of 94.5%, from the coupling between the ^{210}Pb 8^+ seniority isomer and the unpaired proton hole in the $s_{1/2}$ shell.

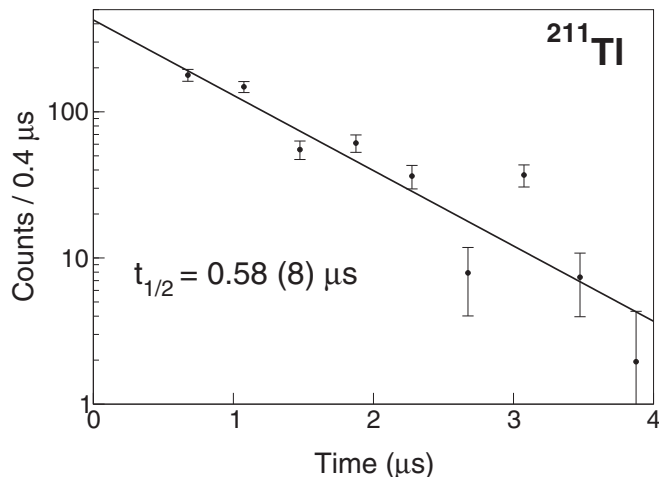


FIG. 4. Time distribution for the 144-keV transition in ^{211}Tl .

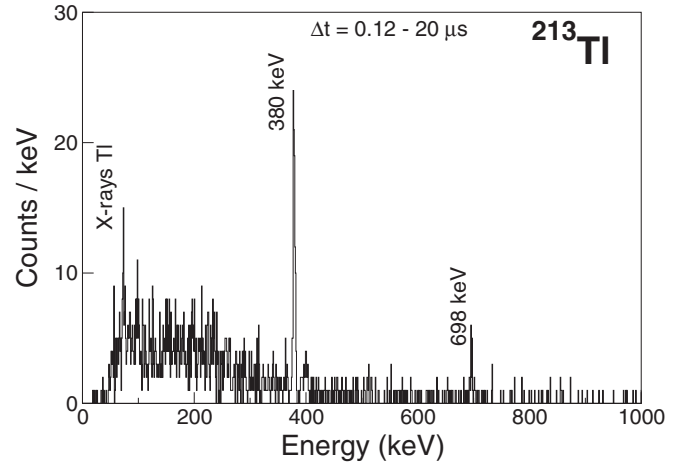


FIG. 5. Gamma-ray spectrum from the decay of the isomeric state in ^{213}Tl . The spectrum has been obtained by selecting a time window of 0.12–20 μs after implantation.

However, the $5/2^+$ state clearly represents a point of disagreement between shell-model calculations and experimental data. Concerning its energy, the nuclear Hamiltonian described above seems to work excellently. The interaction predicts a $5/2^+$ level at 767 keV, in perfect agreement with the recent work in Ref. [5], where spin-parity assignments were fixed and a weak γ -ray line pointed out the existence of a $5/2^+$ state at 736 keV. The discrepancy appears when considering the transition strengths between levels and the resulting branching ratios. The $5/2^+$ state can be fed by an $E2$ transition from the $9/2^+$ level, and by an $E2/M1$ transition from the $7/2^+$ state, the $M1$ being likely dominant in view of the low transition energy. The decay branching ratio from the $9/2^+$ state toward the $7/2^+$ state (also this has to have mainly an $M1$ character) and the $5/2^+$ state was measured in Ref. [5]: 2.6(16)%. This value is very close to our shell-model calculations, which predict 2.8%. On the contrary, for the decay of the $7/2^+$ to the $5/2^+$ and $3/2^+$ levels, our

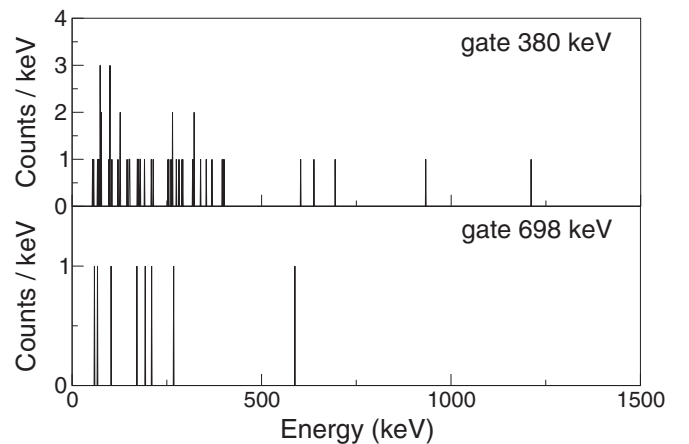


FIG. 6. Gamma-ray spectra in prompt coincidence with the 380- and 698-keV transitions observed in the decay of isomeric states in ^{213}Tl , with gates on the two transitions following the isomers.

TABLE II. Ratio between the ^{213}Tl γ -ray intensities corrected for efficiency and electron conversion, in the hypothesis of $E2$ transitions, and the number of implanted ^{213}Tl ions. The errors on the corrected area are statistical ones quadratically summed to a relative 10% uncertainty in efficiency calibration.

γ energy (keV)	Area	Area corrected/number of ions
380(1)	91 (11)	0.26 (5)
698(1)	17 (5)	0.07 (3)

shell-model predictions fail. From the work in Ref. [5], where no 250-keV γ -ray branching from $7/2^+$ to $5/2^+$ was measured, one can infer an upper limit of 1% for the branching ratio. Our calculations predict a $B(M1 : 7/2^+ \rightarrow 5/2^+)$ strength of $0.014\mu_N^2$ and a $B(E2 : 7/2^+ \rightarrow 3/2^+)$ strength of $135 e^2 \text{fm}^4$, hence a large branching ratio of about 20% for the $7/2^+$ to $5/2^+$ transition. The fact that the decay path of the $7/2^+$ state toward the $5/2^+$ level is much weaker than calculated cannot be easily explained. Here we only point out, as a hint for further work, that if one restricts the proton-hole space to the $s_{1/2}$ shell, than the $B(M1 : 7/2^+ \rightarrow 5/2^+)$ strength becomes vanishing. However, as we shall see later for the ^{211}Tl case, even a large $M1$ suppression would not suffice to justify the nonobservation of the $5/2^+$ state in more neutron-rich isotopes.

In conclusion, limiting to the level energies, the agreement between theory and calculations is quite satisfactory, while for transition rates there is some discrepancy. In this regard, the spectra obtained for $^{211,213}\text{Tl}$ can be regarded as surprising, being a departure from the seniority-like level scheme of ^{209}Tl . We recall here that Pb isotopes do follow the $g_{9/2}$ seniority scheme up to ^{216}Pb [2].

A. Calculations for the ^{211}Tl isotope

When looking at the spectrum in Fig. 2, it is immediately evident that it is different from what was observed in ^{209}Tl . Only one γ line at 144 keV is observed in the spectrum, providing the evidence of the presence of at least one isomer,

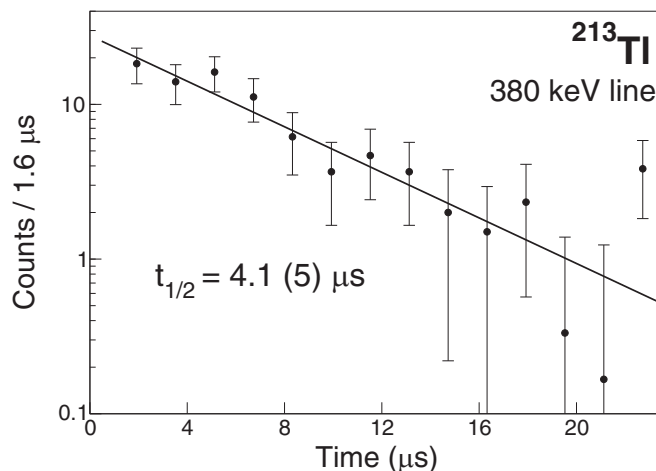


FIG. 7. Time distribution of the 380-keV transition in ^{213}Tl .

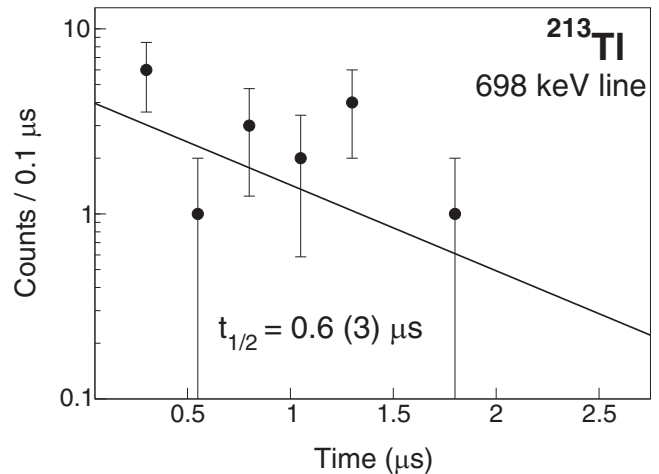


FIG. 8. Time distribution of the 698-keV transition in ^{213}Tl .

with an half-life of $t_{1/2} = (0.58 \pm 0.08) \mu\text{s}$. From the point of view of transition strength, we tentatively assume that the observed γ ray belongs to the γ cascade depopulating a $17/2^+$ isomer. Then, as in ^{209}Tl , the $17/2^+ \rightarrow 13/2^+$ $E2$ transition in ^{211}Tl would be highly converted (thus nondetectable with γ rays), and the $B(E2 : 7/2^+ \rightarrow 3/2^+)$ would range from $(22 \pm 3) e^2 \text{fm}^4$ for $E_\gamma = 20 \text{keV}$ to $(18 \pm 3) e^2 \text{fm}^4$ for $E_\gamma = 80 \text{keV}$. Here it is assumed that the observed half-life originates from the unobserved low-energy $17/2^+ \rightarrow 13/2^+$ $E2$ transition. Following systematics from ^{209}Tl , within the framework of the seniority-scheme, one could suggest that the observed 144-keV transition in ^{211}Tl corresponds to the deexcitation $13/2^+ \rightarrow 9/2^+$, since in ^{209}Tl this transition has a very similar energy of 137 keV. The problem of the nonobservation of the lower-lying levels remains open. In the following, we will show that the transitions between the lower energy levels may not be observed because the 144-keV line could feed an isomer with a long lifetime, outside the observational range of our experiment (about 400 μs).

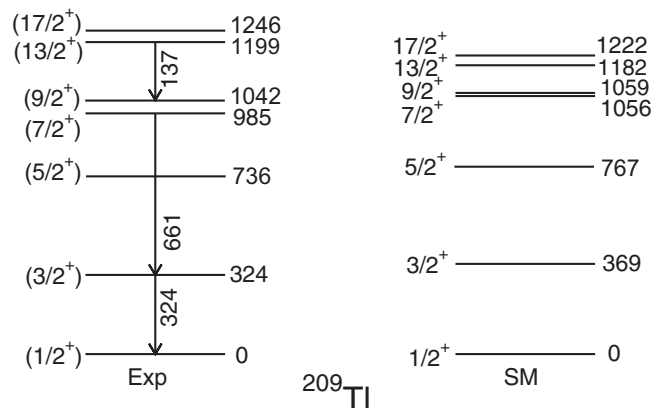


FIG. 9. Experimental [1] and calculated level scheme of ^{209}Tl . The experimental $5/2^+$ state is reported in Ref. [5]. The low-energy transitions depopulating the isomer are taken from the same reference.

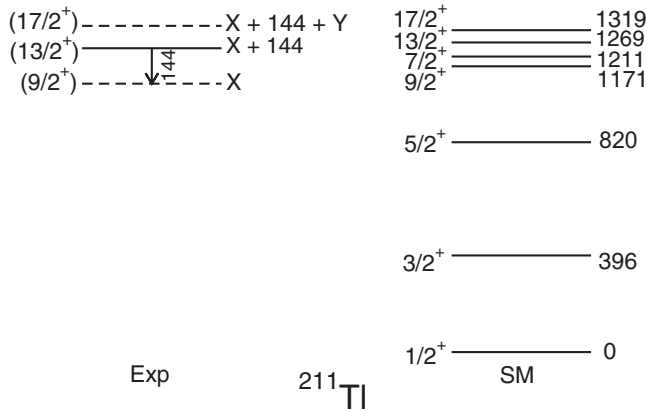


FIG. 10. A tentative proposal for experimental level scheme of ^{211}Tl compared with shell-model calculations performed with the interaction and valence space described in the text.

Shell-model calculations have been performed in the same model space as in the case of ^{209}Tl , and the resulting levels are shown in Fig. 10. In the first place, the calculations suggest that the $17/2^+$ level is isomeric as in ^{209}Tl , due to the low energy of the $E2$ transition to the $13/2^+$ state. This is the same reason why a ^{208}Pb core-breaking study cannot be performed in this case as was done for the lead isotopes. The calculated $B(E2)$ is $34 e^2 \text{fm}^4$ using $e_\pi = 1.5e$ and $e_\nu = 0.8e$, somehow larger than the aforementioned experimental interval of $18\text{--}22 e^2 \text{fm}^4$. The calculated $13/2^+ \rightarrow 9/2^+$ transition energy fits anyway nicely with the 144-keV γ line observed.

In ^{209}Tl , the $9/2^+$ level then decays via a likely predominantly $M1$ transition to the $7/2^+$ state, but shell-model calculations predict that in ^{211}Tl this is no longer possible. The $7/2^+$ level is above the $9/2^+$ level, which thus can only decay to the $3/2^+$ state, neglecting the presence of $5/2^+$ state—see below for further discussion on this point. Incidentally, we remark here that a possible feeding of the $7/2^+$ level via the $13/2^+ \rightarrow 7/2^+$ $E4/M3$ transition is certainly much suppressed in comparison with the $13/2^+ \rightarrow 9/2^+$ $E2$ decay, due to its higher multipolarity and low energy. The $9/2^+ \rightarrow 3/2^+$ decay would then be an $E4/M3$ transition, highly hindered due to its high multipolarity. For a $M3$ character with an energy of 900 keV its Weisskopf single-particle estimate leads to a lifetime of $160 \mu\text{s}$, while for an $E4$ character the estimate is 153 ms. This means that the lifetime for an $E4$ transition is outside the observational limit of the experimental setup. Concerning the $M3$ possibility, a hindrance of the strength of a factor 2 to 3 would be sufficient to make it unobservable as well.

As in the case of ^{209}Tl , the question about the existence of a low-lying $5/2^+$ state, predicted at 820 keV in ^{211}Tl , remains open. The presence of such a state would open a relative fast decay path for the $9/2^+$ state, destroying its supposedly long-lived isomerism. The $9/2^+ \rightarrow 5/2^+$ $E2$ decay should be very suppressed to determine a lifetime larger than $400 \mu\text{s}$ for the $9/2^+$ level, with a $B(E2, 9/2^+ \rightarrow 5/2^+) \lesssim 10^{-4} e^2 \text{fm}^4$.

The conclusion is that shell-model calculations could provide an explanation for the observed level scheme of ^{211}Tl , if one neglects the predicted presence of the $5/2^+$ state. With

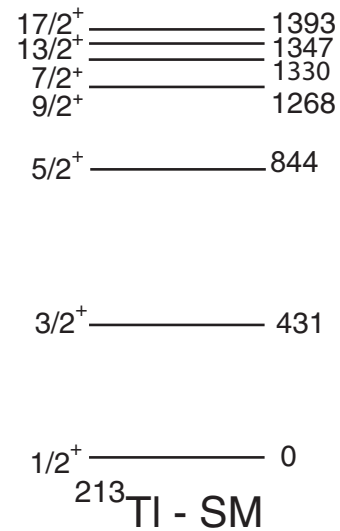


FIG. 11. Shell-model calculations for ^{213}Tl , performed with the interaction and valence space from Ref. [1].

this *caveat*, a $17/2^+$ seniority isomer, as in ^{209}Tl , may be present also in ^{211}Tl . The nonobservation of its full γ -ray cascade to the ground state may be due to the spin trap created by a level inversion between the $9/2^+$ and $7/2^+$ states.

B. Calculations for the ^{213}Tl isotope

The spectrum obtained for ^{213}Tl is different from both ^{209}Tl and ^{211}Tl isotopes, showing one intense γ line of 380 keV, and another weaker line at 698 keV. If one tries to follow the systematics of the seniority scheme, then it is possible that the 380-keV line corresponds to the $3/2^+ \rightarrow 1/2^+$ transition observed with a similar energy in ^{209}Tl . The 698-keV line could then correspond to the $9/2^+ \rightarrow 3/2^+$ γ ray, but its low intensity and the fact that it is not in coincidence with the 380-keV line implies that it is a γ ray connecting two other levels, following another isomer decay. This is further reinforced by the fact the decay time curves of the two γ rays are incompatible within errors. Shell-model calculations were performed also for this nucleus. Figure 11 shows the calculated level scheme, which is very similar to the one obtained for ^{211}Tl .

On the basis of theoretical calculations, one would thus expect ^{213}Tl to be similar to ^{211}Tl , with the same $9/2^+$ state spin trap. This would lead to the observation of a γ -ray cascade similar to ^{211}Tl . Considering that the spectroscopy of ^{213}Tl is radically different, with the presence of two isomers with transition energies not compatible with systematics and shell-model calculations, this may imply that a new low-energy structure appears. The fact the shell-model calculations cannot predict properly the $M1$ transition strength to the observed $5/2^+$ in ^{209}Tl , and to the nonobserved $5/2^+$ in ^{211}Tl , could represent a warning about the real effectiveness of the Hamiltonian employed, especially in describing the proton space and its coupling to the valence neutrons above $N = 126$.

Another key point is the fact that our valence space does not consider $N = 126$, $Z = 82$ core breaking excitations for

neutrons and protons. This precludes the possibility of predicting the energies of intruder configurations, which may become lower in energy when going further from the $N = 126$ shell closure. Similarly, the collective 3^- state of ^{208}Pb cannot be properly described in our model space. It has been predicted that the energy of the collective octupole should become lower beyond $N = 126$ as a result of the strong octupole $g_{9/2}$ - $j_{15/2}$ correlation [23]. Indeed, the presence of a second isomer in ^{210}Hg has also been linked to a possible low-lying octupole state [3]. It cannot be excluded that the observed spectroscopic structure of ^{213}Tl has the same origin.

V. CONCLUSIONS

Isomer-decay γ -ray spectroscopy of neutron-rich $N = 130, 132, ^{211,213}\text{Tl}$ isotopes has been performed. The measured γ -ray spectra show a significant difference with respect to the less exotic ^{209}Tl , at variance with the seniority scheme observed in the $^{210-216}\text{Pb}$ isotopes. Shell-model calculations with a ^{208}Pb core, neutron particles, and proton holes are in good agreement with the ^{209}Tl known level scheme, except for the branching ratios from the $7/2^+$ to the $3/2^+$ and $5/2^+$ states. They show that ^{211}Tl could also have a seniority-scheme-like level structure, but a spin trap along the decay path of the seniority isomers(s) could prevent its observation. In this regard, also the structure of ^{211}Tl can be tentatively described as the coupling of the $d_{3/2}$ and $s_{1/2}$ proton holes to the excited levels observed below the seniority isomers in $^{210-216}\text{Pb}$. As in the case of the ^{209}Tl isotope, the main discrepancy between the shell model employed and the experimental findings concerns the predicted existence of a $5/2^+$ level which is not observed in ^{211}Tl . However, for ^{213}Tl the presence of two distinct isomers, with very different γ -ray intensities, is not explained by our shell-model Hamiltonian,

which would on the contrary suggest that another low-lying structure is appearing, perhaps resembling what has been observed for ^{210}Hg .

In conclusion, the observed isomers in $^{211,213}\text{Tl}$ show a departure from the seniority scheme measured previously in ^{209}Tl and on the even-even $^{210-216}\text{Pb}$ isotopes. Shell-model calculations were performed to try to explain the experimental results, but they fail to reproduce the isomers of ^{213}Tl . From an experimental point of view, it is imperative to gather more data in this region. A first step could be redoing the same measurement presented in this paper but with a much higher statistics to detect possible weak $\gamma\gamma$ coincidences and to better determine lifetimes. A possible future experimental development will be to directly measure the mass of the isomeric states with storage rings [24] in order to measure their absolute energy. From the theoretical point of view, the inclusion of intruder configurations or collective octupole states could help to shed light in what remains one of the less-explored zones of the nuclide chart.

ACKNOWLEDGMENTS

The work of GSI accelerator staff is acknowledged. A.G., M.D., and E.F. acknowledge the support of INFN, Italy, and MICINN, Spain, through the AIC10-D-000568 action. A.G. has been partially supported by MICINN, Spain, and the Generalitat Valenciana, Spain, under Grants No. FPA2008-06419 and No. PROMETEO/2010/101. The support of the UK STFC, of the Swedish Research Council under Contract No. 2008-4240 and of the DFG(EXC 153) is also acknowledged. The experimental activity has been partially supported by the EU under the FP6-Integrated Infrastructure Initiative EURONS, Contract No. RII3-CT-2004-506065 and FP7- Integrated Infrastructure Initiative ENSAR, Grant No. 262010.

-
- [1] N. Al-Dahan *et al.*, *Phys. Rev. C* **80**, 061302(R) (2009).
 - [2] A. Gottardo *et al.*, *Phys. Rev. Lett.* **109**, 162502 (2012).
 - [3] A. Gottardo *et al.*, *Phys. Lett. B* **725**, 292 (2013).
 - [4] C. Ellegaard *et al.*, *Nucl. Phys. A* **259**, 435 (1976).
 - [5] B. M. S. Amro *et al.*, *Phys. Rev. C* **95**, 014330 (2017).
 - [6] R. Caballero-Folch *et al.*, *Phys. Rev. Lett.* **117**, 012501 (2016).
 - [7] R. Caballero-Folch *et al.*, *Phys. Rev. C* **95**, 064322 (2017).
 - [8] Z. Li, Z. Jinhua, Z. Jiwen, W. Jicheng, Q. Zhi, Y. Youngfeng, Z. Chun, J. Genming, G. Guanghui, D. Yifei, G. Tianrui, W. Tongqing, G. Bin, T. Jinfeng, and L. Yixiao, *Phys. Rev. C* **58**, 156 (1998).
 - [9] M. Marouli *et al.*, *Appl. Radiat. Isotopes* **74**, 123 (2013).
 - [10] G. Benzoni *et al.*, *Phys. Lett. B* **715**, 293 (2012).
 - [11] A. I. Morales *et al.*, *Phys. Rev. C* **89**, 014324 (2014).
 - [12] Z. Podolyak, CERN INTC proposal CERN-INTC-2013-046 (2013).
 - [13] A. Gottardo, *Eur. Phys. J. Plus* **129**, 9 (2014).
 - [14] H. Geissel *et al.*, *Nucl. Instrum. Methods B* **70**, 286 (1992).
 - [15] S. Pietri *et al.*, *Nucl. Instrum. Methods B* **261**, 1079 (2007).
 - [16] P. H. Regan *et al.*, *Nucl. Phys. A* **787**, 491 (2007).
 - [17] R. Kumar *et al.*, *Nucl. Instrum. Methods A* **598**, 754 (2009).
 - [18] P. H. Regan *et al.*, *Int. J. Mod. Phys. E* **17**, 8 (2008).
 - [19] E. K. Warburton, *Phys. Rev. C* **44**, 233 (1991).
 - [20] A. Hosaka *et al.*, *Nucl. Phys. A* **444**, 76 (1985).
 - [21] E. Caurier and F. Nowacki, *Acta Phys. Pol. B* **30**, 705 (1999).
 - [22] E. Caurier and G. Martínez-Pinedo, *Nucl. Phys. A* **704**, 60 (2002).
 - [23] I. Hamamoto, *Phys. Rep.* **10**, 63 (1974).
 - [24] M. Reed *et al.*, *Phys. Rev. Lett.* **105**, 172501 (2010).